Development of a Self-Pressurizing Ethane-Nitrous Oxide Propulsion System for an Amateur Rocket

Marcus A. Shelton,[1] and James P. Biaglow.[2]
University of Alabama in Huntsville, Huntsville, Alabama, 35899, United States of America

The propulsion system described in this paper is currently being developed by The Space Hardware Club at The University of Alabama in Huntsville for the 2018 Spaceport America Cup Intercollegiate Rocket Engineering Competition. The development of the propulsion system commenced in July of 2017. The team is currently manufacturing the engine, propellant tanks, and other subsystems while gearing up for an engine hot fire test by April 13, 2018. The propulsion system described in this paper uses a self-pressurizing fuel and oxidizer, ethane and nitrous oxide respectively. The propellants are contained within a 6061-T6 aluminum pressure vessel which contains provisions for propellant fill, drain, vent, and pressure relief. The engine utilizes a single post cavitating venturi oxidizer injector, a simple ethane manifold, and a mixture ratio biased injection faceplate. Gaseous boundary layer cooling is employed as the primary cooling method. Every portion of the rocket has been or will be designed, analyzed, manufactured, and assembled by members of the student team. This paper focuses on the modeling, analysis, and design of components for the engine and fluids system portions of the launch vehicle.

Nomenclature

$\dot{m}$	=	Mass flow rate
μ	=	Viscosity
A	=	Area
C_{cpv}	=	Specific heat at constant pressure
COPV	=	Composite overwrapped pressure vessel
COTS	=	Commercial-off-the-shelf
G_c	=	Film coolant weight flow rate per unit area of chamber surface
h_g	=	Bartz gas-side heat transfer coefficient
IREC	=	Intercollegiate Rocket Engineering Competition
M	=	Mach Number
Pr	=	Prandtl Number
SRAD	=	Student researched and developed
T_{aw}	=	Adiabatic wall temperature
T_{co}	=	Initial film-coolant temp
T_{wg}	=	Maximum gas side wall temp
V	=	Velocity
γ	=	Gas Constant
η	=	Film cooling efficiency
ρ	=	Density
σ	=	Boundary Layer Correction Factor

I. Introduction

WITH 124 teams from around the world expected to gather in New Mexico for the event, The Intercollegiate Rocketry Engineering Competition at the Spaceport America Cup is the largest collegiate rocketry competition in the world. The competition divides projects into six categories based on the selected propulsion system and target apogee. The competition rules allow for COTS solid or hybrid propulsion systems, SRAD solid, hybrid, or liquid propulsion systems, and target apogees of 10,000 or 30,000 ft. The most advanced category requires teams to construct a rocket using an SRAD liquid or hybrid propulsion system to ascend to a target altitude of 30,000 feet above ground level while carrying an 8.8 lb payload.

[1] Undergraduate, Mechanical and Aerospace Engineering Department, mas0050@uah.edu, AIAA Student Member.
[2] Undergraduate, Mechanical and Aerospace Engineering Department, jpb0024@uah.edu, AIAA Student Member.

With many years of experience with COTS solid rocketry, The Space Hardware Club at The University of Alabama in Huntsville has decided to take the leap into SRAD liquid propulsion. In the summer of 2017, preliminary work began on the development of the rocket. The current system model is shown in Fig. 1.

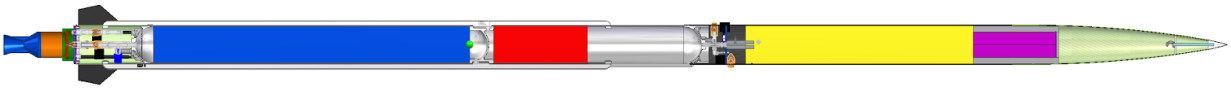

Fig. 1 Overall Rocket Model

The rocket airframe has a nominal outer diameter of 6.125 inches and is approximately 16 feet in length. The dry mass of the rocket is 80 pounds and the wet mass is 129 pounds. The upper airframe contains the recovery system and payload, shown in yellow and purple respectively. The system employs a predictive apogee guidance algorithm to determine engine shutdown time. Other development efforts include a highly functional simulation to assist in the design of the rocket as well as ground support equipment for fill and launch operations. This paper will focus on the propulsion system; containing the Fluids System and the Engine.

II.Fluids System

A. Overview

For the purposes of this paper and project, Fluids System comprises of the launch vehicle's propellant tank, run manifolds, vent manifolds, supercharging manifolds, and the system's interfaces with the airframe, recovery, avionics, and engine. A system block diagram, comprising of the nitrous oxide system and the ethane system, is shown in Fig. 2.

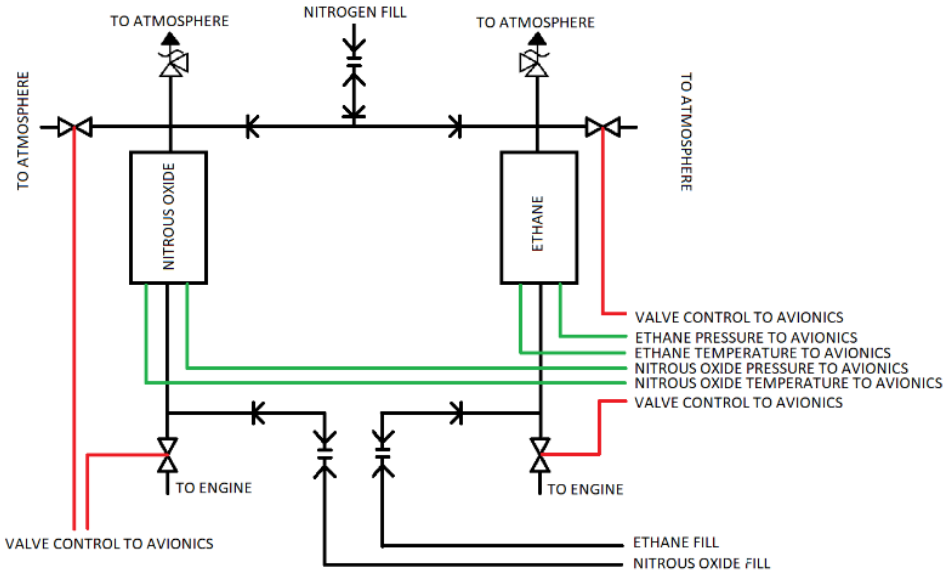

Fig. 2 Fluids System Piping Diagram

While the block diagram depicts two identical individual propellant systems in function and form, the real-world implementation varies as dictated by the launch vehicle requirements. From the 2018 Spaceport America Cup IREC Competition Design, Test, & Evaluation Guide and Rules & Requirements Document, in the event of launch abort, the system must have the ability to safely vent propellant. Additionally, the pressure vessel must be designed to a burst pressure of at least two times the maximum expected operating pressure, must be proof tested to at least one and half times the maximum expected operating pressure, and must have a relief device to open at no greater than proof pressure. From the competition requirements and the team's own design and safety requirements, further requirements were derived and developed. The engine team dictated that the nitrous oxide tank volume must be 1,404 cubic inches and the ethane tank volume must be 819 cubic inches. Both propellant volumes allow for a 15% ullage volume above the liquid propellant level. It was also determined that the system must contain provisions for measuring propellant

level, pressure, and temperature. These requirements were used to drive the design towards its current configuration. The current configuration of the fluids system is shown in Fig. 3.

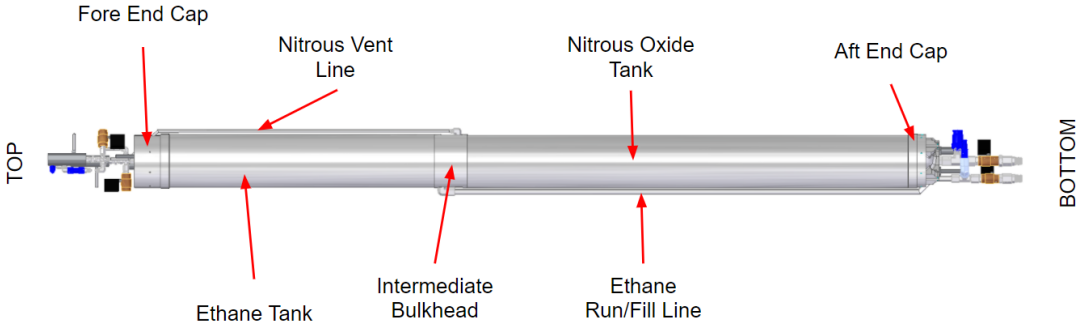

Fig. 3 Fluids System Overview

As shown in Fig. 3, the pressure vessel is fully aluminum and contains both propellants separated by a common hemispherical intermediate bulkhead. When viewing the rocket in the vertical orientation, the ethane tank is located above the nitrous oxide tank. This configuration was chosen because the nitrous oxide injector is located along the central axis of the engine, the nitrous oxide has larger mass flow rate requirements, and the ethane is less susceptible to decomposition or ignition within the propellant lines. Located above the pressure vessel are the vent manifolds for each respective propellant as well as the nitrogen manifold which is used to supercharge both propellants prior to motor ignition. The vent manifolds are used to vent the propellants to atmospheric temperature and to provide pressure relief in the case of ground support equipment failure or overpressure within the pressure vessel. At the bottom of the pressure vessel are the nitrous and ethane run manifolds which deliver propellants to the engine and serve as the fill location for the tanks. On each end of the propellant tanks, there is a pressure and temperature sensor which is used to monitor each propellant's real time conditions. Propellant tank fill levels are monitored indirectly by a load cell which measures rocket mass on the launch rail or test stand.

B. Propellant Properties

An extensive trade study was completed to determine the most appropriate engine cycle and propellants. The engine cycles considered were the gas-generator, pressure fed, and blowdown cycles. Due to the aggressive timeline, limited team experience, and limited budget, the gas-generator cycle was quickly eliminated from consideration. Choosing between the pressure fed and blowdown cycles was slightly less obvious because this trade was also coupled with the propellant trade and selection. Ultimately, the blowdown cycle was chosen because it was shown to deliver the greatest performance within the limitations of the competition rules and the small scale of the rocket.

The main propellants combinations considered were N2O/Propane, N2O/Kerosene, LOx/Kerosene, H202/Kerosene, and N20/Ethane. Due to the handling and engineering complexities involved with cryogenic propellant and the added mass and complexity involved with an onboard pressurant, N2O and ethane were chosen as the ideal propellants for the rocket. As shown in Fig. 4, both propellants have very similar pressure-temperature curves which make them an ideal pair for use in a blowdown engine.

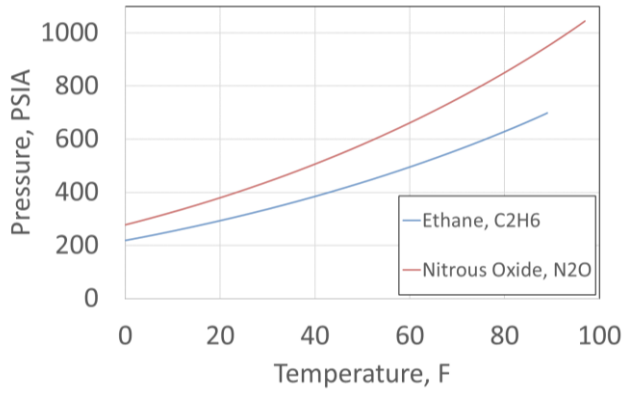

Fig. 4 Pressure vs. Temperature for Ethane and Nitrous Oxide [1]

Due to the high vapor pressure of N_2O and Ethane, both propellants will continuously boil off throughout flight to maintain a high pressure within the propellant tanks. Although the propellants will boil throughout flight, the boil off rate will not completely match the use rate, resulting in a pressure decrease throughout engine burn. To mitigate the pressure reduction, prior to flight, both propellants ullage cavities will be supercharged to the tank's maximum operating pressure using high pressure nitrogen. Using a nitrogen supply from the launch vehicle's ground support equipment, nitrogen will be flowed into the propellant tanks moments prior to engine ignition. As shown in Fig. 5, the propellant tank model calculates that a major performance limiting drop in pressure will not be realized throughout the flight. The steep pressure drop off at the end is representative of engine run valve cutoff by the launch vehicle's guidance, navigation, and control algorithms. These algorithms will be used to ensure that the launch vehicle does not overshoot the target apogee of 30,000 feet AGL. After the nitrous oxide valve is shut, ethane will be vented through the engine and nitrous oxide will be vented through the vent manifold.

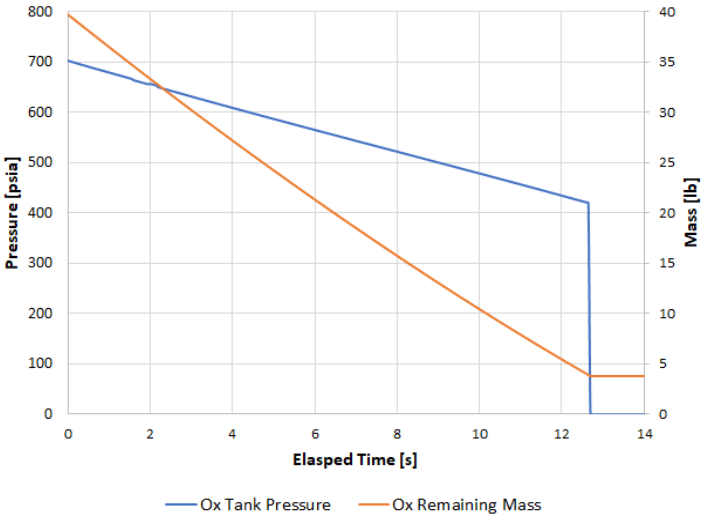

Fig. 5 Nitrous Oxide Tank Pressure and Mass vs. Burn Time

C. Pressure Vessel

To store the propellants, it was realized that one or more pressure vessels would be required. COTS options were considered, but no commercially available pressure vessels fit the pressure, diameter, volume, and weight requirements for the rocket. The manufacturing options considered were: fully composite, COPV, and aluminum. Since the club doesn't currently have filament winding capabilities and the competition rules dictated that a factor of safety of three was required for composite pressure vessels while only a factor of safety of two was required for aluminum, it was determined that an aluminum pressure vessel would be the lightest and easiest to manufacture option for the given operating conditions. Aluminum alloy 6061-T6 was chosen for its cost, availability, weldability, and strength.

Based on the propellant properties, it was determined that a maximum operating pressure near 1,000 psig would be ideal. Keeping in mind the competition required factor of safety of two and the team-imposed 6 inch outer diameter constraint, Eq. (1) for thin wall pressure vessel hoop stress was rearranged into Eq. (2) to solve for required tube thickness. In both equations, σ represents hoop stress in pounds per square inch, P represents the gage pressure in pounds per square inch, D represents the mean diameter in inches, and t represents the wall thickness in inches. Assuming the ultimate tensile strength of 6061-T6 aluminum to be 45,000 psi, the required wall thickness was calculated to be 0.130 inch. Since the closest COTS aluminum tube wall thickness is 0.125 inch and 0.1875 inch, the lower pressure rating of the 0.125 inch wall thickness was chosen versus the added weight or lengthy turning operation of the 0.1875" wall thickness. Using 0.125 inch wall thickness tubing results in a maximum operating pressure of 957 psig.

$$\sigma = \frac{PD}{2t} \tag{1}$$

$$t = 2\left(\frac{3P}{P+\sigma}\right) \tag{2}$$

As shown in Fig. 6, a horizontal band saw was used to cut the cylinder for the ethane pressure vessel to a length of 30 inches and the cylinder for the nitrous pressure vessel to a length of 50 inches.

Fig. 6 Pressure Vessel Cylinder on Horizontal Band Saw

The end caps for the propellant tanks were also designed using thin wall pressure vessel hoop stress equations. However, due to manufacturing limitations and design constraints, all three pressure vessel caps vary greatly from an ideal hemispherical geometry. Consequently, the stress and deflection of the end caps were verified using Nastran finite element analysis. Plots of the worst-case deflection and Von Mises stress experienced by the hemispherical intermediate bulkhead are shown in Fig. 7 where the maximum Von Mises stress was 20,400 psi and the maximum deflection was 0.008 inch. The results for the Nitrous Oxide and Ethane end caps were similar to the results for the intermediate bulkhead. All of the calculated results confirmed the results of the hoop stress equation and showed that the factor of safety of two would be met.

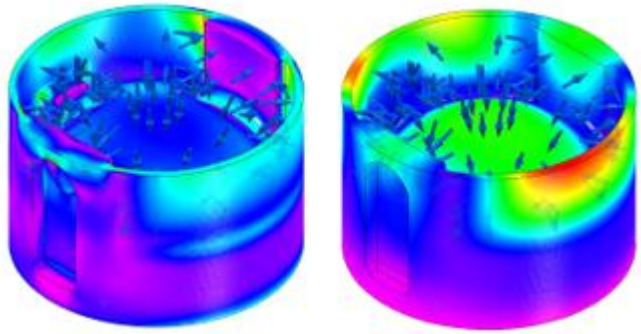

Fig. 7 Von Mises Stress (left) and Deflection (right) for 1,000 psi ethane, 0 psi nitrous oxide loading

Manufacturing of the end caps is currently being completed by team members in the Mechanical and Aerospace Engineering Machine Shop using a Haas VF-1 CNC Mill and Haas TL-1 CNC Lathe. In-process pictures of the ethane end cap are shown in Fig. 8.

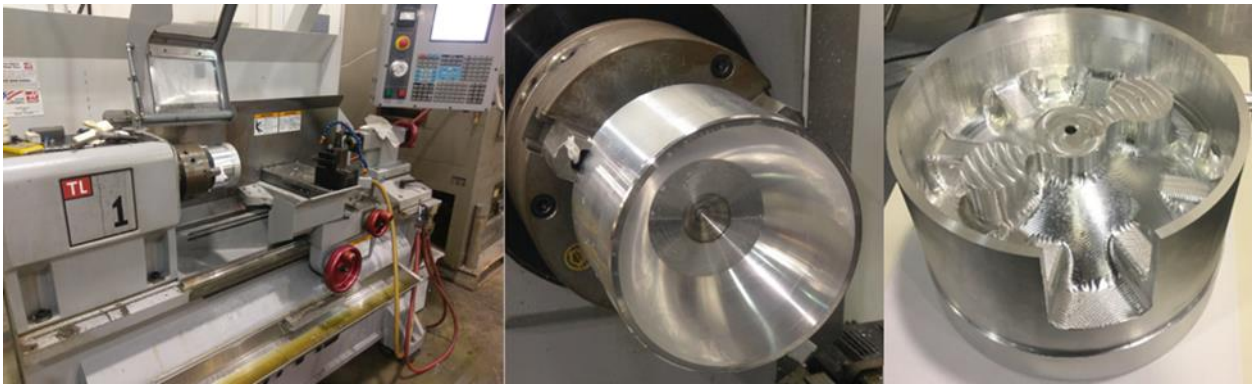

Fig. 8 Ethane End Cap on CNC Lathe (left and center) and Finished (right)

Once the Ethane end cap, Nitrous Oxide end cap, and intermediate bulkhead manufacturing is complete, all fives pieces of the pressure vessel will be welded together using a set of circumferential welds at the joints between each piece. The welds will be completed by an experienced welder using a gas tungsten arc welding, or TIG welding, process. Due to the welding process, it is anticipated that the heat affected zone of the weld will be significantly weakened by localized annealing. To return the material strength back to pre-weld levels, the entire pressure vessel will undergo a heat treatment and precipitation hardening process. Pressure vessel and fluid system performance will be verified through a series of tests including hydrostatic pressure testing to one and half times the expected operating pressure and visual leak down tests with liquid leak detector.

D. Piping and Instrumentation

To control propellant flow, pressure, and safety, a series of piping manifolds were created throughout the rocket. The diametrically largest manifold is the Nitrous Oxide run manifold which has an internal diameter of 0.5 inch and flows directly from the nitrous oxide pressure vessel into the engine nitrous oxide injector. The diametrically second largest manifold is the ethane run manifold which has an internal diameter of 0.375 inch and flows out of the side of the intermediate bulkhead, down the side of the pressure vessel, and into the engine ethane manifold. These diameters were chosen for their respective propellants by balancing the mass flow rate requirements, line velocities, and system mass. Equation (3), where $\dot{m}$ is mass flow rate, ρ is fluid density, and A is tubing internal cross-sectional area, was used to determine velocity, V, in the lines. Assuming both propellants are at their respective vapor pressure and 80 degrees Fahrenheit, the nitrous oxide will have a line velocity of 39.2 feet per second and the Ethane will have a line velocity of 45.3 feet per second. Ref. 2 and Ref. 3 were used to verify that the chosen tube diameter, line velocity, pressures, temperatures, materials and configuration would not force the Nitrous Oxide to operate above autoignition or decomposition limits. A strict cleaning and storage procedure will be followed to eliminate or reduce contamination within the Nitrous Oxide system.

$$V = \frac{\dot{m}}{\rho * A} \tag{3}$$

In order to produce high quality simulations of engine performance, the pressure drops through the Nitrous Oxide run manifold and Ethane run manifold were calculated using a combination of Eq. (4), Eq. (5), Eq. (6), and Eq. (7) shown below. First, the Reynold's numbers were calculated for each propellant based on line velocity, v, the hydraulic diameters, d_h, and the dynamic viscosity, v. Next, the Darcy-Weisbach friction factor, f, was iteratively calculated using the Colebrook-White Equation where ε represents absolute roughness of the pipe. Then, the major head loss was calculated where L is the pipe length and g represents the acceleration due to gravity. Next, minor head losses were calculated where K represents the loss coefficient for pipe fittings, unions, entrances, exits, and other features. Loss coefficients were found in Ref. 4. Finally, all of the head losses were summed together and converted to psi values for the pressure loss between the propellant vessel and the engine. The pressure drops through the Nitrous Oxide and Ethane manifolds were calculated to be 17 psi and 25 psi, respectively.

$$Re = \frac{u * d_h}{v} \tag{4}$$

$$\frac{1}{\sqrt{f}} = -2 * \log\left(\frac{\varepsilon}{3.7 * d_h} + \frac{2.51}{Re\sqrt{f}}\right) \tag{5}$$

$$H_{major} = f * \frac{L}{d_h} * \frac{u^2}{2g} \quad (6)$$

$$H_{minor} = K * \frac{u^2}{2g} \quad (7)$$

Both the nitrous oxide and ethane run manifolds contain engine run valves and propellant filling provisions. Although Nitrous oxide and Ethane manifold use different size valves, both valves use the same basic design. Each run valve uses a ball valve which has been modified to allow for a digital servo to turn the valve using a custom four bar linkage. As designed, the valves are expected to transition from the fully closed position to the fully open position in 0.15 seconds. Valve position is verified using a set of limit switches. A model of the 0.5" servo-actuated ball valve is shown in Fig. 9.

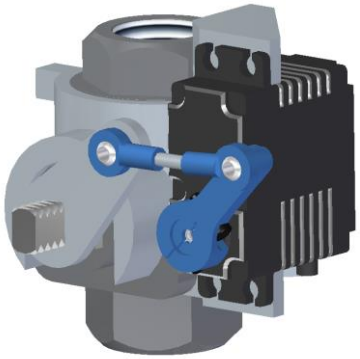

Fig. 9 Servo-Actuated Ball Valve Assembly

Also located within the ethane and nitrous oxide run manifolds are a check valve and hydraulic quick disconnect which allow for filling the pressure vessel with propellants. Prior to flight, an actuator on the ground support equipment releases the quick disconnects from the side of the rocket. The use of an actuated quick disconnect allows for personnel to be a safe distance away from the rocket during all fill and launch operations.

At the top of the rocket, the vent and nitrogen manifolds share many of the characteristics found on the run manifolds. The vent manifolds use 0.25 inch servo-actuated ball valves along with burst discs set to 1.5 times the maximum expected operating pressure. The nitrogen fill manifold uses the same quick disconnect found on the lower portion of the rocket and check valves are used to ensure that the propellants do not mix. All fittings within the manifold are made from 316 stainless steel and a variety of fittings types were used including AN/JIC, NPT, and BSPP. All tubing is made from aluminum which traded favorably when compared to stainless steel with respect to weight and cost. For instrumentation, each pressure vessel chamber is equipped with a stainless-steel T type thermocouple and a 0-1,500 psi pressure transducer.

III. Engine

A. Overview

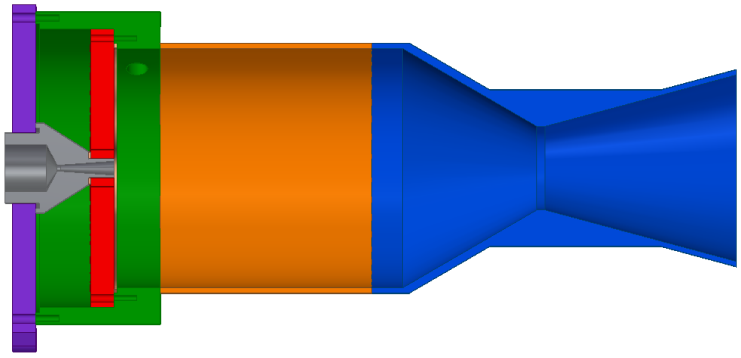

Fig. 10 'Workhorse' Engine CAD

Bearing in mind the budgetary, scheduling, and technical constraints, simplicity was the guiding principle for the engine design. Fig. 10 shows CAD of the engine that will be used to conduct initial hot fire testing, known as the workhorse testing article. The engine features a single oxidizer injector, colored in silver, that connects directly to the N_2O feed system. This post is wedged between the engine cap, shown in purple, and the injection faceplate, shown in red. The injector faceplate is in turn bolted into the injector housing, pictured in green. The injector faceplate, injector housing, and the engine cap together form the ethane manifold. The parts in orange and blue are the combustion chamber and nozzle, respectively, making up the thrust chamber assembly. The engine utilizes gaseous boundary layer film cooling and mixture ratio biasing as the primary cooling methods. The flight configuration will necessitate a tertiary cooling method that will be designed after hot fire data is obtained and is therefore not presented in this overview.

Table 1 Engine Parameters

Propellants	N2O & C2H6
Thrust	810 lbs
Isp	211 s
c* (85% eff)	4,570 ft/s
Area Ratio	5
Chamber Pressure	500 psia
Thrust Coefficient	1.48
O/F	7

B. Injector Design

Conventional large liquid rocket engines employ either impinging, pintle or coaxial injector designs. Impinging injectors require a liquid-liquid stream of fuel and oxidizer to collide, creating small droplets of the mixed propellants; something unable to insure as the Ethane fuel will be gaseous at injection. Pintle types are effective for throttling engines, a feature not needed in this engine; so design began on coaxial injectors. However, after the intricacy and fabrication load of 17 individual assemblies was fully in view, this design was scrapped for the single post injector design discussed in this study.

This change affects most parts of the engine. The use of only one oxidizer element eliminates the need for an oxidizer manifold altogether. In turn, the lack of multiple oxidizer downcomers eliminated the need for complex swirl post fuel sleeves that surrounded the oxidizer posts and were replaced with simple straight hole orifices on the injector faceplate. This simplification of the system saves weight, eases sealing concerns and significantly reduces the fabrication work load. The two main features of the injector design to be discussed in this paper are the flow design through the oxidizer post and the mixture ratio bias thermal mitigation technique that will be discussed in the thermal section.

1. Cavitating Venturi Oxidizer Post

A cavitating venturi is a flow regulating device that mostly decouples mass flow rate from downstream conditions by forcing the static pressure of the flow to below the vapor pressure of the liquid, resulting in the formation of vapor bubbles. The two fundamental concepts for understanding this process are cavitation and Bernoulli's Equation. The latter concept states that in an incompressible, inviscid flow the total pressure, or stagnation pressure, is equal to the sum of the static pressure and dynamic pressure. Therefore, as the flow velocity increases, the dynamic pressure increases and the static pressure decreases. If the static pressure decreases to equal or below the vapor pressure of the fluid, some of the fluid will turn to vapor, or cavitate. As this gas is released, the density of the two-phase flow will decrease, thus decreasing the dynamic pressure and increasing the static pressure. Once the static pressure returns to above the vapor pressure, the liquid will cease cavitating and an equilibrium will be reached. This phenomenon is utilized in a cavitating venturi injector. Without cavitation, a decrease or increase in the pressure drop across the injector would mean an increase or decrease in the mass flow rate, respectively. In a cavitating circumstance, however, a change in pressure drop corresponds to a change in the amount of cavitation, not mass flow rate. Therefore; after a critical pressure drop is reached, the mass flow rate becomes constant. A cavitating venturi injector utilizes a

converging-diverging section of tubing to induce cavitation at or above a critical flow point. This design can be seen in Fig. 11. Much of this modelling and test verification was shown in Ref. 6 for use in a hybrid rocket oxidizer injector.

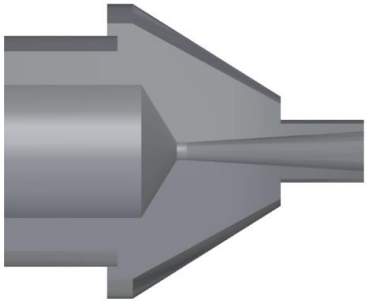

Fig. 11 Cavitating Venturi Oxidizer Post CAD

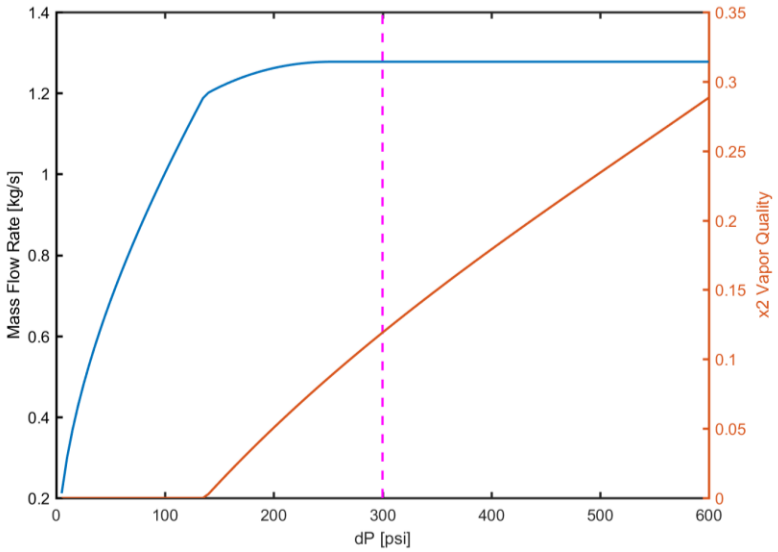

Fig. 12 Mass Flow Rate at Given Pressure Drops

This phenomenon provides two major benefits to the development of the engine. The first is that a known constant mass flow rate greatly simplifies mathematical modeling of the properties of the engine. Designing models and geometries based on the assumption of a constant mass flow rate is far easier than designing to a time-variant mass flow rate schedule. In Fig. 12, a graph of the mixture quality and mass flow rate is given. Note the quasi-linear increase in quality as the pressure drop increases, indicating that more liquid is cavitating as well as the pink dotted line indicating a critical mass flow rate. The primary function of the venturi design is to mostly decouple the feed line system and the combustion chamber, virtually eliminating feed-line coupled instabilities. When the mass flow rate varies with the pressure fluctuations of the chamber, the system becomes prone to coupled fluctuations that result in wild jumps in chamber pressure and mass flow rates, often leading to catastrophic failures of the system.

B. Thermal Modelling and Heat Mitigation

In any liquid rocket engine, thermal mitigation is of paramount importance. The core combustion temperature of ethane and nitrous oxide is around 3750 °F given an O/F of 7, far hotter than the combustion chamber wall could support. Thus, several cooling methods must be employed. Currently, the primary cooling method for the engine is boundary layer cooling and mixture ratio biasing. Additional cooling methods such as ablative inserts, thermal coating and secondary injection sites might be necessary pending hot fire data.

The main operating principle of both primary cooling methods is to reduce the temperature of the gas in contact with the wall of the combustion chamber. Because the magnitude of the heat flux into the chamber wall is dependent on the temperature of the gas in the chamber, the total heat flux into the chamber wall is reduced.

1. Boundary Layer Cooling and Thermal Model

This section will discuss the method of boundary layer cooling as well as providing a small overview of the thermal model. These two things aren't coupled arbitrarily. The governing equation for the boundary layer calculations are intrinsically linked into the thermal model. The foundations of the thermal model are given in ref. 5. There are three fundamental equations, Eqs. (8), (9), & (10).

$$\frac{T_{aw}-T_{wg}}{T_{aw}-T_{co}} = e^{-\left(\frac{h_g}{G_c C_p \eta_c}\right)} \tag{8}$$

$$h_g = \left[\frac{0.026}{D_t^{0.2}}\left(\frac{\mu^{0.2}C_p}{Pr^{0.6}}\right)_{ns}\left(\frac{(p_c)_{ns}g}{c^*}\right)^{0.8}\left(\frac{Dt}{R}\right)^{0.1}\right] * \left(\frac{A_t}{A}\right)^{0.9}\sigma \tag{9}$$

$$\sigma = \frac{1}{\left[\frac{1}{2}\frac{T_{wg}}{(T_c)_{ns}}\left(1+\frac{\gamma-1}{2}M^2\right)+\frac{1}{2}\right]^{0.68}\left[1+\frac{\gamma-1}{2}M^2\right]^{0.12}} \tag{10}$$

Eq. (8) shows the equation used to find the temperature of the layer of gas in contact with the wall given an amount of boundary layer coolant injected. Boundary layer cooling is the process by which a coolant, usually the fuel, to form a layer of insulation to reduce the temperature in contact with the wall, a property known as gas-side wall temperature. In the exponent of equation two, the Bartz correlation, h_g, is used. This correlation was defined by Bartz to simplify the convective heat transfer in a rocket thrust chamber. To solve this equation, the propellent properties, such as specific heat and Prandtl Number taken from NASA CEA and thrust chamber geometries are used to find this correlation. Sigma is a correction factor for the changing properties of the gas in contact with the wall as it moves across the boundary layer. Notice that in calculating the value of sigma, the value for the wall-side gas temperature is needed. Yet referring to Eq. (8), the gas-side wall temperature is the value that needs to be solved. Therefore, the implicit solution for the gas side wall temperature must be solved iteratively. This iterative loop sits at the center of the heat model that also accounts for heat transfer from the wall to the atmosphere as well as other sources of heat transfer to better predict the temperature of the wall.

To validate this model, hot fire data must be obtained. Hot fire testing data will allow for the actual gas-side wall temperature and heat fluxes at discrete stations during the workhorse hot fire campaign. This information will better inform decisions about potential tertiary cooling methods.

2. Mixture Ratio Biasing

As noted above, the boundary layer cooling acts as an insulation layer between the core combustion and the wall. The higher the temperature of the core combustion, the more heat transferred to the boundary layer equating to more heat transferred to the wall. It follows, then, that by decreasing the temperature of the gases in contact with the boundary layer, the heat transferred to the wall will be decreased. This is the operating principle of mixture ratio biasing. Mixture ratio biasing is when the mixture ratio, and thus combustion temperature, is reduced as the radius from the central axis increases. This is accomplished by controlling the amount of fuel injected in specific locations in the combustion chamber

Table 2 Injection Zone Parameters

Zone	Hole Diameter (inches)	Number of Holes	Mass Flow Rate (lb/s)
1 (Blue)	0.038	16	0.236
2 (Green)	0.018	24	0.079
Boundary Layer (Yellow)	0.018	50	0.157

Fig. 13 Injector Faceplate Cross Section CAD

In Fig. 13, a cross section of the fuel injector faceplate is pictured. The central hole is where the oxidizer post is held and the holes on the outside of the yellow zones are the bolt holes that connect the injector faceplate to the ethane manifold. In blue, the zone 1 core combustion injectors are pictured. Around 75% of core combustion fuel is injected in this zone. Notice that the orifices in this zone are cut at a 13-degree angle. This better focuses the fuel flow into the path of the oxidizer flow, ensuring that the most intense combustion occurs as far from the chamber wall as possible. Zone 2 injectors are noted in the green boxes. The remaining 25% of the core combustion fuel is injected through this zone. This fuel combusts with the oxidizer not burned in the core combustion at a mixture ratio of around 3, though this number is a rough estimation. The orifices noted in yellow are the boundary layer cooling holes.

This method of reducing wall temperature is simple yet requires hot fire testing to verify biased area combustion temperature. The calculation of the effective mixture ratio is not as simple as the total oxidizer flow divided by the total fuel flow, as the boundary layer cooling does not factor into this calculation. Additionally, the effective mixture ratio in contact with the boundary layer must be found to obtain the properties of the combustion gasses needed in the heat modeling calculations.

IV. Acknowledgments

The authors would like to thank the University of Alabama in Huntsville College of Engineering, the Alabama Space Grant Consortium, National Space Club Huntsville, Blue Origin, the UAH Office of the Vice President of Research, the UAH College of Science, the UAH Honors College, the UAH Department of Physics and Astronomy, the Joseph Moquin Endowment, Advanced Circuits, Advanced Heat Treat Corp., and the UAH Student Government Association for their generous support towards the numerous projects conceptualized, designed, built, and flown by the UAH Space Hardware Club. The authors would also like to thank the following people and organizations for their assistance:

Dr. Francis Wessling and Dr. Brian Landrum for serving as advisors on this paper
The UAH Space Hardware Club
The entire SHC Spaceport America Cup team

The first author would also like to thank Adam Bower for his patience and mentorship.

V.References

[1] National Institute of Standards and Technology, Chemistry WebBook, SRD 69, *Thermophysical Properties of Fluid Systems*, URL: http://webbook.nist.gov/chemistry/fluid/ [Retrieved 11 November, 2017]
[2] Kramer, A. F., et al., Summary of Nitrous Oxide Investigations, AFWL-TR-75-231, Air Force Weapons Laboratory, Air Force Systems Command, Kirtland Air Force Base, New Mexico, July, 1976
[3] Rhodes, G. W., Investigation of Decomposition Characteristics of Gaseous and Liquid Nitrous Oxide, AD-784802, Air Force Research Lab, Kirtland Air Force Base, New Mexico, July, 1974.
[4] Hodge, B. K., and Taylor, R. P., *Analysis and Design of Energy Systems 3rd Edition*, Prentice Hall, New Jersey, 1998.
[5] Huzel, D. K., and Huang, D. H., *Modern Engineering for Design of Liquid-Propellant Rocket Engines*, AIAA, 1992.
[6] Waxman, B. S., Cantwell, B., Alonso Juan José, and Zilliac, G. G., "An investigation of injectors for use with high vapor pressure propellants with applications to hybrid rockets," dissertation, 2014.